Journal of Inorganic Biochemistry 103 (2009) 1579–1584

Contents lists available at ScienceDirect

Journal of Inorganic Biochemistry

journal homepage: www.elsevier.com/locate/jinorgbio

Demonstration of aluminum in amyloid fibers in the cores of senile plaques in the brains of patients with Alzheimer's disease

Sakae Yumoto [a,*], Shigeo Kakimi [b], Akihiro Ohsaki [c], Akira Ishikawa [c]

[a] Yumoto Institute of Neurology, Kawadacho 6-11, Shinjuku-ku, Tokyo 162-0054, Japan
[b] Faculty of Medicine, Nihon University, Ohyaguchiuemachi 30-1, Itabashi-ku, Tokyo 173-8610, Japan
[c] College of Humanities and Sciences, Nihon University, Sakurajousui 3-25-40, Setagaya-ku, 156-8550 Tokyo, Japan

ARTICLE INFO

Article history:
Received 10 April 2009
Received in revised form 3 July 2009
Accepted 7 July 2009
Available online 15 August 2009

Keywords:
Alzheimer's disease
Aluminum
Beta-amyloid peptide
Senile plaque core
Energy-dispersive X-ray spectroscopy (EDX)
Senile plaque

ABSTRACT

Aluminum (Al) exposure has been reported to be a risk factor for Alzheimer's disease (senile dementia of Alzheimer type), although the role of Al in the etiology of Alzheimer's disease remains controversial. We examined the presence of Al in the Alzheimer's brain using energy-dispersive X-ray spectroscopy combined with transmission electron microscopy (TEM-EDX). TEM-EDX analysis allows simultaneous imaging of subcellular structures with high spatial resolution and analysis of small quantities of elements contained in the same subcellular structures. We identified senile plaques by observation using TEM and detected Al in amyloid fibers in the cores of senile plaques located in the hippocampus and the temporal lobe by EDX. Phosphorus and calcium were also present in the amyloid fibers. No Al could be detected in the extracellular space in senile plaques or in the cytoplasm of nerve cells. In this study, we demonstrated colocalization of Al and beta-amyloid (Abeta) peptides in amyloid fibers in the cores of senile plaques. The results support the following possibilities in the brains of patients with Alzheimer's disease: Al could be involved in the aggregation of Abeta peptides to form toxic fibrils; Al might induce Abeta peptides into the beta-sheet structure; and Al might facilitate iron-mediated oxidative reactions, which cause severe damage to brain tissues.

1. Introduction

Aluminum (Al) is a highly neurotoxic element that can cause nerve cell degeneration in the brains of humans and experimental animals [1,2]. Al exposure has been proposed as a risk factor for Alzheimer's disease (senile dementia of Alzheimer type; AD), although the role of Al in the pathogenesis of AD remains controversial [3–7]. The accumulation of Al in the nuclei of nerve cells and in neurofibrillary tangles has been demonstrated in the AD brain by histochemical staining [8–10], laser microprobe mass analysis [11], secondary ion mass spectrometry [12] and particle-induced X-ray emission (PIXE) analysis [13].

However, the accumulation of Al in senile plaques in the AD brain has long been disputed. It is to be noted that senile plaques are one of the pathological hallmarks of AD [14] and the core of the senile plaque mainly consists of aggregates of beta-amyloid (Abeta) peptides [15–17].

In 1986, Edwardson et al. measured high concentrations of Al (4–19%) and silicon (Si; 6–24%) in the isolated cores of senile plaques using energy-dispersive X-ray spectroscopy (EDX) combined with scanning electron microscopy (SEM-EDX) [18,19], whereas Jacobs et al. and Tokutake et al. failed to detect Al in senile plaques in the AD brain by SEM-EDX [20,21]. Landsberg et al. also failed to demonstrate the presence of Al in senile plaque cores by microprobe PIXE analysis [22]. They concluded that the Al previously detected in isolated senile plaque cores [18,19] was the result of contamination by Al silicates, which were the main components of the dust in the air. On the other hand, Beauchemin and Kisilevsky detected Al in isolated senile plaques cores from the AD brain using inductively coupled plasma mass spectrometry [23]. Recently, Collingwood et al. isolated fragments of senile plaque cores (approximately 1–2 μm in diameter, round or oval in shape) from frozen cortical brain tissues of AD patients and demonstrated Al in half of these isolated plaque core fragments by EDX combined with transmission electron microscopy (TEM-EDX) analysis [24]. In contrast, Walton detected no Al in the cores of senile plaques using a novel histochemical method that clearly stained Al in the nuclei of nerve cells and neurofibrillary tangles in the AD brain [10].

In this study, we evaluated the presence of Al in the brains (hippocampus and temporal lobe) of patients with AD using TEM-EDX. TEM-EDX analysis allows simultaneous imaging of subcellular structures with high spatial resolution and analysis of small quantities of elements contained in the same subcellular structures.

* Corresponding author. Tel./fax: +81 3 3341 3406.
E-mail addresses: yumoto-s@viola.ocn.ne.jp (S. Yumoto), akihiro@phys.chs.nihon-u.ac.jp (A. Ohsaki), ishiaki1@gmail.com (A. Ishikawa).

0162-0134/$ - see front matter © 2009 Published by Elsevier Inc.
doi:10.1016/j.jinorgbio.2009.07.023

2. Materials and methods

2.1. Chemicals

Potassium dichromate, ammonium molybdate, HEPES, ethanol, and propylene oxide were purchased from Wako Pure Chemicals Industries, Ltd., Osaka, Japan. Epon, 25% glutaraldehyde, and 20% formaldehyde, carbon rods, Formvar, and nylon mesh were obtained from Nisshin EM Co. Ltd., Tokyo, Japan. Al di-stearate was purchased from Soekawa Chemical Co., Ltd., Tokyo, Japan. All buffers, fixatives, and staining solutions were prepared with Milli-Q water (Milli-Q Plus System, Millipore, Mississauga, Canada).

2.2. PIXE analysis of chemicals

In order to ensure the accurate measurements of Al in the samples by TEM-EDX, it is important to exclude contamination by exogenous Al and to rule out the presence of elements that have energy levels resulting in characteristic X-rays similar to that of Al Kα. PIXE analysis simultaneously detects Al with high sensitivity and demonstrates the presence of elements with energy levels resulting in characteristic X-ray similar to that of Al Kα [25]. All chemicals used for TEM-EDX analysis, including carbon rods, Formvar films, and small blocks of Epon were examined by PIXE analysis. Saturated potassium dichromate solution, saturated ammonium molybdate solution, and saturated HEPES solution (total 0.1 ml each) were mounted on Formvar films, and dried in a vacuum evaporator for PIXE analysis. Ethanol, propylene oxide, 25% glutaraldehyde, and 20% formaldehyde were placed in a small, concave Teflon dish (total 1.0 ml each) and were dried for PIXE analysis. The PIXE spectra of these samples were measured at the accelerating voltage of 3 MeV using a tandem accelerator at Micro Analysis Laboratory of Tokyo University.

2.3. Standard samples for analytical electron microscopy

2.3.1. Formvar films

Formvar films were mounted on nylon mesh and coated with evaporated carbon.

2.3.2. Epon and Al-Epon mixtures

Al di-stearate was mixed with Epon to homogeneity and used to make Al standards that contain 100 ppm Al, 50 ppm Al, 25 ppm Al, and 12.5 ppm Al. Because Al di-stearate is a highly hydrophobic compound, homogeneous Al-Epon mixtures can be prepared easily. Epon and Al-Epon mixtures were hardened in an oven maintained at 60 °C. Thin sections (0.1-μm thick) of these Epon and Al-Epon mixtures were cut using an LKB Ultrotome microtome equipped with a diamond knife, mounted on nylon mesh, and coated with evaporated carbon. Glass knives were not used for sample sectioning, because glass contains considerable amounts of Al and Si.

2.4. Preparation of brain samples for TEM-EDX analysis

Brain tissues (hippocampus and temporal lobe) were removed at autopsy from five patients (76–85 years old) with AD using a clean stainless steel knife. After the brain tissues were transferred to a clean room, the cutting surface at autopsy was cut off using a sharp, clean stainless steel knife and the arachnoid membrane was removed. Autopsy instruments were rinsed in 70% ethanol overnight, washed with ethanol, rinsed in Milli-Q water, dried, and kept in a clean box before use. Instruments were changed between each autopsy.

Samples from hippocampal region CA1 and the temporopolar area of the superior temporal gyrus (Brodmann area 38) were collected from each patient for this study. The tissue samples were cut into small blocks, fixed with 3% glutaraldehyde and 2.5% paraformaldehyde in 0.1 M HEPES buffer (pH 7.2) for 12 h, washed with 10% sucrose in the same buffer for 1 h, and post-fixed with 3% glutaraldehyde and 2.5% potassium dichromate in 0.1 M HEPES buffer (pH 7.6) for 3 h. Samples were dehydrated with an ascending series of ethanol, substituted with propylene oxide, embedded into Epon using a clean plastic capsule with a cap, and hardened at 60 °C. From the brain of each patient, 40–60 Epon blocks were prepared. Thick sections (approximately 1-μm thick) were cut using an LKB Ultrotome microtome equipped with a diamond knife. Thick sections were stained with 5% toluidine blue to examine the presence of senile plaques in the sections by light microscopy. When senile plaques could not be observed in the sections, thick sections were further cut from the same block to locate senile plaques for the preparation of thin sections. Thin sections (0.1-μm thick) were cut using an LKB Ultrotome microtome equipped with a diamond knife, mounted on nylon mesh, stained with 2% ammonium molybdate, and coated with evaporated carbon. In each patient, approximately 80–120 thin sections were prepared from the hippocampus and from the temporal lobe, respectively. These thin sections were stored in a clean desiccator, and used as samples for TEM-EDX analysis.

Osmium (Os) tetroxide is the standard fixative used to prepare biological samples for electron microscopy. However, the energy levels of characteristic X-ray of Al Kα (Kα-1, 1.48670 keV and Kα-2, 1.48627 keV) and those of Os Mξ (Mξ-1, 1.4919 keV and Mξ-2, 1.4831 keV) are so close that they cannot be distinguished between each other by EDX analysis [26]. It is to be noted that the energy resolution of EDX was approximately 77.1 eV at 1.486 keV. Therefore, we used potassium dichromate instead of Os tetroxide as a fixative to enhance electron density of the samples.

Epon was used in this study, because Epon is highly resistant to electron beams and thin sections of Epon can be easily cut with a diamond knife. The brain samples were fixed in Teflon bottles and dehydrated in Teflon beakers to avoid Al contamination from laboratory glasswares. Additionally, all solutions including fixatives, buffers, and staining solutions were stored in Teflon bottles. All the procedures for the preparation of samples for TEM-EDX analysis were carried out in a clean room.

2.5. TEM-EDX analysis

EDX spectra of samples and standards were measured using a TN 5502 X-ray microanalyser (Noran Instruments Inc., Middleton, USA) combined with a JEM 2000EX transmission electron microscope (JEOL Ltd., Tokyo, Japan). Analyses were made on standard samples and brain samples from the patients with AD. Senile plaques in the brain samples were identified by TEM and electron beams were irradiated to a small spot (approximately 0.2 μm in diameter) in these samples at an accelerating voltage of 100 keV and the emitted X-rays were analysed with the X-ray microanalyser.

3. Results

3.1. PIXE analysis of chemicals used for the sample preparation

PIXE analysis of the chemicals used for the preparation of samples revealed no Al or other elements with energy levels resulting in characteristic X-ray close to that of Al Kα.

3.2. Standard samples

No Al was detected in Formvar films or thin sections of Epon by TEM-EDX analysis (Figs. 1 and 2). High peaks for Si, Fe, and Cu were detected in Formvar films and in Epon sections (Figs. 1 and 2). It is

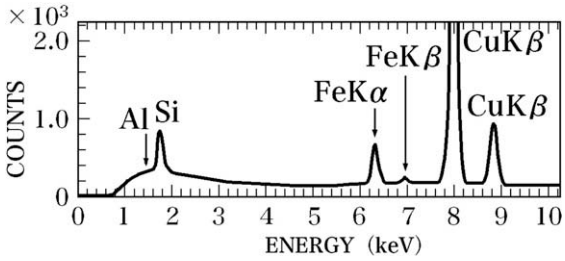

Fig. 1. EDX spectrograph of a Formvar film. No Al (arrow) could be detected in the Formvar film by TEM-EDX analysis. High peaks of Si, Fe, and Cu were demonstrated. It is noteworthy that Si, Fe, or Cu could not be de demonstrated in Formvar films by PIXE analysis.

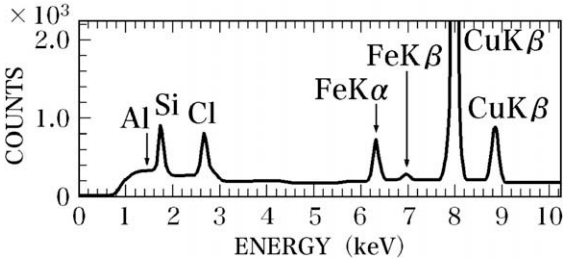

Fig. 2. EDX spectrograph of an Epon section. No Al (arrow) could be detected in the thin section (0.1-μm thick) of Epon. High peaks of Si, Fe, Cu, and Cl were observed. The Cl peak seems to be derived from the Epon itself. The peaks of Fe and Cu could have originated from the components of the electron microscope. The Si peak could have resulted from contamination from oil vapor evaporated from the vacuum pump oil.

noteworthy that peaks corresponding to Si, Fe, or Cu could not be demonstrated in Formvar films or in Epon by PIXE analysis. PIXE analysis has a higher sensitivity than TEM-EDX analysis in the detection of elements including Al, Si, Fe, and Cu [25]; however, when a certain element is present in the pathway of electron beams in TEM-EDX analysis, large amount of characteristic X-ray of this element will be produced by the irradiation of electron beams. Therefore, it is possible that the high peaks of Fe and Cu observed in Formvar films and in Epon sections measured by TEM-EDX may have originated from the Fe and Cu used in the components of the electron microscope. Since the vacuum oil provided for the electron microscope contained large amounts of Si, the Si peak observed in the analysis of Formvar films and Epon may have resulted from contamination from oil vapor evaporated from the vacuum pump oil.

In addition to the peaks for Si, Fe, and Cu, a chlorine (Cl) peak was detected from Epon sections by TEM-EDX analysis (Fig. 2). Kametani detected Cl in thin sections of Epon by EDX analysis [27]. The Cl peak measured in the Epon sections seems to be derived from the Epon itself. The peaks of Si, Cl, Fe, and Cu in the Epon sections were so high that TEM-EDX could not be applied to the analysis of these elements in brain samples.

An Al Kα peak was detected in Al-Epon sections containing 12.5 ppm of Al. When the Al concentration in the Al-Epon mixture was elevated from 12.5 ppm to 25 ppm, 50 ppm, or 100 ppm, the heights of Al Kα peaks increased almost proportionally to the increase in Al concentration.

3.3. Senile plaques

Senile plaques in thick sections were clearly stained with toluidine blue by light microscopy. Although only limited regions of the brain were examined, there was a trend toward a greater number of senile plaques in the hippocampus (region CA1) in comparison to the temporal lobe (temporopolar area of the superior temporal gyrus); additionally, the number of senile plaques increased with age. These findings seem to be consistent with previously reported results [28]. A senile plaque usually contained about 3–8 small-sized cells with a round nucleus, resembling microglial cells. No nerve cells were detected in the proximity of senile plaques.

Senile plaques with cores were identified in thin sections of brain samples using TEM. Fig. 3 shows an electron micrograph of a core of a senile plaque in the hippocampus fixed with potassium dichromate. A large number of electron-dense amyloid fibers ran radially from the center of the core toward the periphery. The amyloid fibers were about 0.2 μm in diameter, and longitudinal striations were occasionally observed on the amyloid fibers. These morphological features of cores fixed with potassium dichromate observed in this study were identical to those of cores fixed with Os tetroxide [29]. The cores of senile plaques in the hippocampus and in the temporal lobe were structurally similar by TEM.

When the amyloid fibers in the cores of senile plaques (Fig. 4A, arrow) were examined by EDX, an Al Kα peak was clearly demonstrated (Fig. 4B). Peaks of phosphorus (P) and calcium (Ca) were also detected in the amyloid fibers in the hippocampus and in the temporal lobe. Al peaks were detected both in the central region of the core and in amyloid fibers situated in the intermediate and peripheral regions of the core.

In the brain samples of each patient, at least five cores in the hippocampus and five in the temporal lobe were examined by TEM-EDX. It is to be noted that Al was demonstrated in all the cores that were analysed. The concentrations of Al in amyloid fibers in senile plaques located in both the hippocampus and in the temporal lobe ranged from approximately 35–50 ppm (Table 1). No age-related differences in Al concentrations in amyloid fibers were observed. In contrast, no Al was detected in the extracellular space in the senile plaques (Fig. 5A and B) or in the cytoplasm of nerve cells by TEM-EDX.

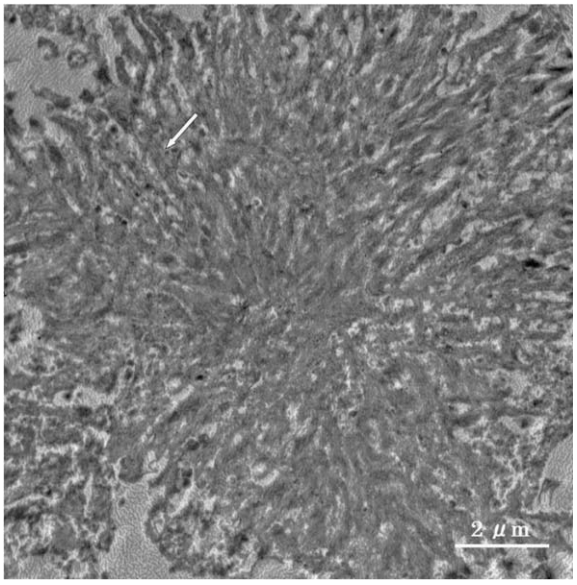

Fig. 3. Electron micrograph of a core of a senile plaque observed in the hippocampus. A large number of amyloid fibers ran radially from the center of the core toward the periphery. The amyloid fibers were about 0.2 μm in diameter, and longitudinal striations were occasionally observed on the amyloid fibers (arrow). The AD brain was fixed with potassium dichromate and stained with ammonium molybdate.

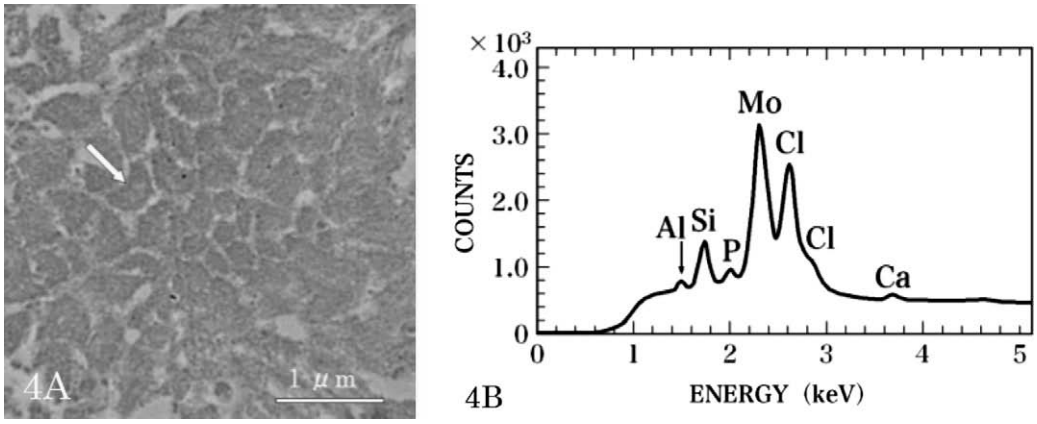

Fig. 4. Electron micrograph (4A) and EDX spectrograph (4B) of an amyloid fiber in the core of senile plaque in the temporal lobe. The amyloid fiber (A, arrow) was examined by EDX. An Al Kα peak was clearly demonstrated (B) in the amyloid fiber. Peaks of P and Ca were also detected in the amyloid fiber. The brain was fixed with potassium dichromate and stained with ammonium molybdate.

Table 1
Al concentrations in amyloid fibers in senile plaque cores.

Patients	Age	Hippocampus (ppm)		Temporal lobe (ppm)	
		Mean ± SD	*n*	Mean ± SD	*n*
Case 1	76	41.8 ± 3.3	5	40.4 ± 2.8	5
Case 2	79	44.3 ± 4.1	5	45.1 ± 4.5	5
Case 3	81	42.5 ± 3.8	5	40.1 ± 3.2	5
Case 4	82	43.8 ± 4.1	5	42.3 ± 3.6	5
Case 5	85	42.0 ± 3.7	5	43.9 ± 3.9	5

Al concentrations (ppm) in amyloid fibers in the cores of senile plaques located in the hippocampus and in the temporal lobe are expressed as mean ± standard deviation (SD). *n*: The number of amyloid fibers analysed in this study.

Microglial cells were often observed close to the cores of senile plaques located in the hippocampus and in the temporal lobe. These microglial cells possessed a number of lysosomes with an electron-dense substance filling their cytoplasm. Peaks of Al, P, and Ca were also observed in the lysosomes (Fig. 6A, arrow) of microglial cells by EDX (Fig. 6B). The patterns of the peaks of Al, P, and Ca in the lysosomes were similar to those analysed in amyloid fibers in the cores. It has been reported that these microglial cells phagocytose amyloid fibers in the core into their lysosomes [30–32]. Therefore, it is likely that the Al detected in the lysosomes originated from the Al in amyloid fibers of the core.

4. Discussion

The results from this study demonstrated the presence of Al in amyloid fibers in the cores of senile plaques located both in the hippocampus and in the temporal lobe by TEM-EDX analysis. It is to be noted that no Al was detected in the extracellular space in senile plaques (Fig. 5), or in the cytoplasm of nerve cells by TEM-EDX. Contamination by dust (mainly Al silicates) can be excluded by the observation of samples using TEM, as most of the dust in the air has a diameter of 0.4–4 μm [22] whilst the spatial resolution of the transmission electron microscope used in this study was about 0.2 nm. In addition, since Al was not detected by PIXE analysis in the chemicals used for the sample preparation in TEM-EDX analysis, it is reasonable to rule out exogenous Al contamination of the brain samples in this study. PIXE analysis also demonstrated that the chemicals used for the sample preparation did not contain elements that show energy levels of characteristic X-rays close to those of Al Kα.

Collingwood et al. demonstrated Al in isolated plaque core fragments (approximately 1–2 μm in diameter) by TEM-EDX analysis [24]. These authors reported the presence of a circular specialized structure (approximately 0.4–1 μm in diameter) in the center of the core fragments by TEM and by electron tomography. Collingwood et al. did not describe the original location of the isolated plaque core fragments in the core of senile plaques, which were reported to be approximately 10–20 μm in diameter [29]. Since both

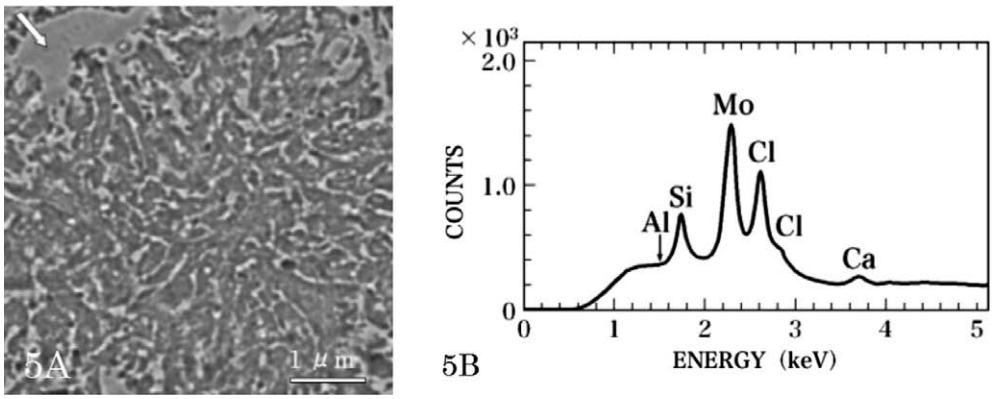

Fig. 5. Electron micrograph (5A) and EDX spectrograph (5B) of the extracellular space adjacent to a core of a senile plaque in the hippocampus. The extracellular space (A, arrow) close to the core of senile plaque was examined by EDX (B). No Al was detected in the extracellular space.

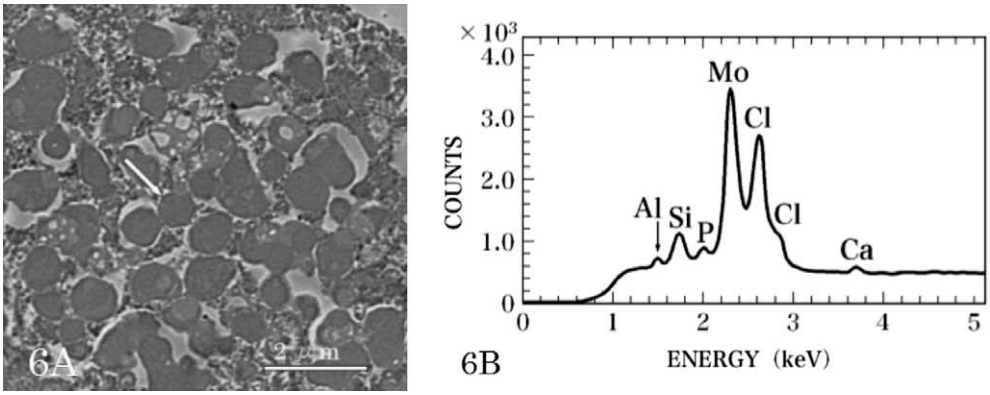

Fig. 6. Electron micrograph (6A) and EDX spectrograph (6B) of a microglial cell near the core of senile plaque in the temporal lobe. The microglial cell possesses a large number of lysosomes with an electron-dense substance in the cytoplasm. The lysosome (A, arrow) was examined using EDX analysis (B). Peaks of Al, P, and Ca were also demonstrated in the lysosome. The patterns of the peaks of Al, P, and Ca in the lysosome in the microglial cell were similar to those analysed in the amyloid fibers in the cores.

the peripheral region and intermediate region of senile plaque cores exclusively consist of amyloid fibers about 0.2 μm in diameter, these amyloid fibers have no room to contain the circular structure 0.4–1 μm in diameter (Fig. 3). Therefore, we speculate that the isolated plaque core fragments reported by Collingwood et al. may have originated from the central region of senile plaque cores. Collingwood et al. reported that Al was detected in approximately 50% of isolated plaque core fragments, which may have originated from the central region of senile plaque cores. In contrast, we demonstrated Al in 100% of all regions of the senile plaque cores examined, including the central region, intermediate region, and peripheral region of the senile plaque cores.

Although both the number of senile plaques and Al concentrations in the brain increase with aging [33–35], no age-related correlations of Al concentrations in amyloid fibers in the cores were observed (Table 1). In addition, the number of senile plaques in the hippocampus is larger than that in the temporal lobe [28]. However, Al concentrations of amyloid fibers located in the hippocampus and those present in the temporal lobe showed approximately similar values. The reason amyloid fibers in the cores showed similar Al concentration values despite age differences or different areas in the AD brain could not be clarified in this study. However, it is interesting to note that microglial cells phagocytose amyloid fibers in the core into their lysosomes [30–32] and that Al was also demonstrated in the lysosomes in this study. Therefore, it is likely that senile plaques may not be the "trash box" to store toxic waste materials or inert residual bodies, but senile plaques may have the function to actively disintegrate toxic materials in the AD brain. DeWitt et al. reported that astrocytes regulate microglial phagocytosis of senile plaque cores of the AD brain [36].

Several authors have reported that formalin fixation has the potential to leach elements including Al from tissues after prolonged durations ranging from 1 week to several years [37–39]. However, we fixed brain tissues with 2.5% glutaraldehyde and 2% formaldehyde at a neutral pH for only 15 h. Gellein et al. concluded that the degree of leaching of elements from tissues was strongly time-dependent. However, Meldrum reported that an increase in Al concentration in formalin solution could be detected immediately after mixing formalin and tissues. Although it is to be noted that these authors did not use a radioisotope of Al [37–39]. Therefore, it is difficult to determine whether the increased Al concentration in formalin solution originated from the Al contained in tissues or from contamination by exogenous Al.

In contrast, it is noteworthy that the solubility of Al is very low, especially at neutral pH. Additionally, Al binds firmly to phosphate, carboxylate, and catecholate groups of proteins, nucleic acids, membranes, cytoskeletons, and chromatin. The ligand exchange rate of Al is the smallest among metals present in tissues [40]. Therefore, we consider it unlikely for the Al in tissues to become solubilized into formalin solution after a short-term formalin fixation especially at neutral pH.

The presence of Al in the cores of senile plaques has been controversial for a long time [18–23]. One of the reasons may be that Al in amyloid fibers in the core could not be stained histochemically [10], while Al in the neurofibrillary tangles and nuclei of nerve cells in the AD brain is stained clearly by histochemistry [8–10]. It seems probable that Al in the core may be embedded deeply in the interior of amyloid fibers. Accordingly, the dyes used in histochemistry could not access the Al within amyloid fibers. It seems likely that Al does not attach to the surface of amyloid fibers in the core after the aggregation of Abeta peptides, but that Al binds with Abeta peptides during the course of aggregation of Abeta peptides, or just before the aggregation.

It is widely recognized that monomers of Abeta peptides aggregate into toxic fibrils (or toxic oligomers) that kill neurons and consequently play a key role in the etiology of AD [41,42]. Amyloid fibers in the core have been reported to consist mainly of the aggregates of Abeta peptides that have a beta-sheet structure [17,43]. In this study, Al was demonstrated to be colocalized with Abeta peptides by TEM-EDX analysis. We hypothesize that colocalization of Al and Abeta peptides in amyloid fibers in the core indicates that Al–Abeta peptide complexes are also present in the extracellular space outside senile plaques before their deposition in the core. Therefore, the results of this study may support the following three possibilities regarding the role of Al in the development of AD.

The first possibility is that Al is involved in the aggregation of Abeta peptides *in vivo* in the AD brains. Since Al (Al^{3+}) is a trivalent cation, Al can interact with acidic groups of the peptides, and bind these peptides with one another [40,44,45]. It has been reported that Al ions promote aggregation of physiological concentrations of Abeta peptides *in vitro* [46]. House et al. and Khan et al. also reported that Al ions accelerate the formation of amyloid fibrils *in vitro* [47,48].

The second possibility is that Al causes the conformational change of Abeta peptides into the beta-sheet structure *in vivo*. Ricchelli et al. reported that Al induces the structural modification of Abeta peptides enriched in beta-sheet conformations *in vitro* [49]. Exley pointed out that only Al and Fe, but not Cu or zinc, are involved in the formation of beta-sheet structure of Abeta peptides [50]. It has also been proposed that Abeta peptides containing beta-sheet structure are directly incorporated into membranes,

forming Ca-permeable ion channels, and causing elevation of intracellular Ca levels and death of nerve cells [51–53].

The third possibility is that Al promotes oxidative injury to brain tissues by facilitating Fe-mediated oxidation reaction in the Alzheimer's brain. Fe is involved in the formation of free hydroxyl radicals via Fenton chemistry, which cause deleterious effects in brain tissues [54,55]. It has been reported that Fe accumulates in the cores of senile plaques [24,56,57] and that deposition of Abeta peptides facilitates the generation of reactive oxygen species in the presence of Fe *in vitro* [58–60]. Xie et al. reported that Al can facilitate Fe-mediated oxidative injury in cultured neurons [61]. In addition, Khan et al. reported that Al potentiates the Fe(II)/Fe(III) redox cycle in favor of Fe(II) *in vitro* [62]. These authors suggested that oxidative damage in the vicinity of senile plaques may be the result of Fenton reactions catalysed by the codeposition of Abeta peptides with Fe and Al.

In conclusion, we demonstrated the colocalization of Al and Abeta peptides in amyloid fibers in the cores of senile plaques using TEM-EDX. P and Ca were also detected in amyloid fibers in the core. The results of this study support the possibility that Al, in cooperation with Abeta peptides, may play an important role in the pathogenesis of AD.

5. Abbreviations

Abeta	beta-amyloid
AD	Alzheimer's disease
EDX	energy-dispersive X-ray spectroscopy
PIXE	particle-induced X-ray emission
SEM	scanning electron microscopy
TEM	transmission electron microscopy

References

[1] A.C. Alfrey, G.R. LeGendre, W.D. Kaehny, New Engl. J. Med. 294 (1976) 184–188.
[2] U. De Boni, J.W. Scott, D.R. Crapper, Histochemistry 40 (1974) 31–37.
[3] D.R. Crapper, S.S. Krishnan, S. Quittkat, Brain 99 (1976) 67–80.
[4] D.R. McLachlan, P.E. Fraser, E. Jaikaran, W.J. Lukiw, in: L.W. Chang (Ed.), Toxicology of Metals, CRC Press, New York, 1996, pp. 387–404.
[5] D.R. McLachlan, C. Bergeron, J.E. Smith, D. Boomer, S.L. Rifat, Neurology 46 (1996) 401–405.
[6] S. Yumoto, H. Nagai, K. Kobayashi, A. Tamate, S. Kakimi, H. Matsuzaki, J. Inorg. Biochem. 97 (2003) 155–160.
[7] V. Rondeau, H. Jacqmin-Gadda, D. Commenges, C. Helmer, J.F. Dartigues, Am. J. Epidemiol. 169 (2009) 489–496.
[8] R.W. Shin, V.M. Lee, J.Q. Trjanowski, Histol. Histopathol. 10 (1995) 969–978.
[9] H. Murayama, R.W. Shin, J. Higuchi, S. Shibuya, T. Muramoto, T. Kitamoto, Am. J. Pathol. 155 (1999) 877–885.
[10] J.R. Walton, Neurotoxicology 27 (2006) 385–394.
[11] P.F. Good, D.P. Perl, L.M. Bierer, J. Schmeidler, Ann. Neurol. 31 (1992) 286–292.
[12] S. Yumoto, S. Kakimi, H. Matsushima, A. Ishikawa, Y. Homma, in: A. Fisher, I. Hanin, M. Yoshida (Eds.), Progress in Alzheimer's and Parkinson's Diseases, Plenum Press, New York, 1998, pp. 293–300.
[13] S. Yumoto, Y. Horino, Y. Mokuno, S. Kakimi, K. Fujii, Nucl. Instrum. Meth. B 109/110 (1996) 362–367.
[14] A. Alzheimer, Z Neurol. Psychiat. 4 (1911) 356–385.
[15] D.J. Selkoe, C.R. Abraham, M.B. Podlisny, L.K. Duffy, J. Neurochem. 46 (1986) 1820–1834.
[16] S. Ikeda, D. Allsop, G.G. Glenner, Prog. Clin. Biol. Res. 317 (1989) 313–323.
[17] J. Dong, C.S. Atwood, V.E. Anderson, S.L. Siedlak, M.A. Smith, G. Perry, P.R. Carey, Biochemistry 42 (2003) 2768–2773.
[18] J.A. Edwardson, J. Klinowski, A.E. Oakley, R.H. Perry, J.M. Candy, Ciba Found. Symp. 121 (1986) 160–179.
[19] J.M. Candy, A.E. Oakley, J. Klinowski, T.A. Carpenter, R.H. Perry, J.R. Atack, E.K. Perry, G. Blessed, A. Fairbairn, J.A. Edwardson, Lancet 327 (1986) 354–357.
[20] R.W. Jacobs, T. Duong, R.E. Jones, G.A. Trapp, A.B. Scheibel, Can. J. Neurol. Sci. 16 (Suppl. 4) (1989) 498–503.
[21] S. Tokutake, H. Nagase, S. Morisaki, S. Oyanagi, Neurosci. Lett. 185 (1995) 99–102.
[22] J.P. Landsberg, B. McDonald, F. Watt, Nature 360 (1992) 65–68.
[23] D. Beauchemin, R. Kisilevsky, Anal. Chem. 70 (1998) 1026–1029.
[24] J.F. Collingwood, R.K. Chong, T. Kasama, L. Cervera-Gontard, R.E. Dunin-Borkowski, G. Perry, M. Pósfai, S.L. Siedlak, E.T. Simpson, M.A. Smith, J. Dobson, J. Alzheimers Dis. 14 (2008) 235–245.
[25] S.A.E. Johansson, J.L. Campbell, PIXE: A Novel Technique for Elemental Analysis, John Wiley and Sons, Chichester, 1988.
[26] J.A. Bearden, Rev. Mod. Phys. 39 (1967) 78–124.
[27] K. Kametani, J. Electron Microsc. 51 (2002) 265–274.
[28] H. Braak, E. Braak, Acta Neuropathol. 82 (1991) 239–259.
[29] J. Wegiel, H.M. Wisniewski, Acta Neuropathol. 81 (1990) 116–124.
[30] K.H. el Hachimi, J.F. Foncin, C.R. Acad. Sci. III 317 (1994) 445–451.
[31] M.R. D'Andrea, G.M. Cole, M.D. Ard, Neurobiol. Aging 25 (2004) 675–683.
[32] T. Bolmont, F. Haiss, D. Eicke, R. Radde, C.A. Mathis, W.E. Klunk, S. Kohsaka, M. Jucker, M.E. Calhoun, J. Neurosci. 16 (2008) 4283–4292.
[33] J.R. McDermott, A.I. Smith, K. Iqbal, H.M. Wisniewski, Neurology 29 (1979) 809–814.
[34] W.R. Markesbery, W.D. Ehmann, T.I. Hossain, M. Alauddin, D.T. Goodin, Ann. Neurol. 10 (1981) 511–516.
[35] H. Shimizu, T. Mori, M. Koyama, M. Sekiya, H. Ooami, Nippon Ronen Igakkai Zasshi 31 (1994) 950–960.
[36] D.A. DeWitt, G. Perry, M. Cohen, C. Doller, J. Silver, Exp. Neurol. 149 (1998) 329–340.
[37] V.J. Bush, T.P. Moyer, K.P. Batts, J.E. Parisi, Clin. Chem. 41 (1995) 284–294.
[38] R.D. Meldrum, J. Biomed. Mater. Res. 57 (2001) 59–62.
[39] K. Gellein, T.P. Flaten, K.M. Erikson, M. Aschner, T. Syversen, Biol. Trace Elem. Res. 121 (2008) 221–225.
[40] B. Martin, Ciba Found. Symp. 169 (1992) 5–25.
[41] D.M. Walsh, D.J. Selkoe, Protein Pept. Lett. 11 (2004) 213–228.
[42] D.M. Walsh, D.J. Selkoe, J. Neurochem. 101 (2007) 1172–1184.
[43] C.L. Shen, G.L. Scott, F. Merchant, R.M. Murphy, Biophys. J. 65 (1993) 2383–2395.
[44] S. Yumoto, H. Nagai, H. Matsuzaki, H. Matsumura, W. Tada, E. Nagatsuma, K. Kobayashi, Brain Res. Bull. 55 (2001) 229–234.
[45] Y.R. Chen, H.B. Huang, C.L. Chyan, M.S. Shiao, T.H. Lin, Y.C. Chen, J. Biochem. 139 (2006) 733–740.
[46] P.W. Mantyh, J.R. Ghilardi, S. Rogers, E. DeMaster, C.J. Allen, E.R. Stimson, J.E. Maggio, J. Neurochem. 61 (1993) 1171–1174.
[47] E. House, J. Collingwood, A. Khan, O. Korchazkina, G. Berthon, C. Exley, J. Alzheimers Dis. 6 (2004) 291–301.
[48] A. Khan, A.E. Ashcroft, V. Higenell, O.V. Korchazhkina, C. Exley, J. Inorg. Biochem. 99 (2005) 1920–1927.
[49] F. Ricchelli, D. Drago, B. Filippi, G. Tognon, P. Zatta, Cell. Mol. Life Sci. 62 (2005) 1724–1733.
[50] C. Exley, J. Alzheimers Dis. 10 (2006) 173–177.
[51] M. Kawahara, Curr. Alzheimer Res. 1 (2004) 87–95.
[52] H. Jang, J. Zheng, R. Nussinov, Biophys. J. 93 (2007) 1938–1949.
[53] D. Drago, A. Cavaliere, N. Mascetra, D. Ciavardelli, C. di Ilio, P. Zatta, S.L. Sensi, Rejuvenation Res. 11 (2008) 861–871.
[54] K. Honda, G. Casadesus, R.B. Petersen, G. Perry, M.A. Smith, Ann. NY Acad. Sci. 1012 (2004) 179–182.
[55] R.J. Castellani, P.I. Moreira, G. Liu, J. Dobson, G. Perry, M.A. Smith, X. Zhu, Neurochem. Res. 32 (2007) 1640–1645.
[56] J.R. Connor, S.L. Menzies, S.M. St Martin, E.J. Mufson, J. Neurosci. Res. 31 (1992) 75–83.
[57] M.A. Smith, P.L.R. Harris, L.M. Sayres, G. Perry, Proc. Natl. Acad. Sci. 94 (1997) 9866–9868.
[58] B.J. Tabner, S. Turnbull, O.M. El-Agnaf, D. Allsop, Free Radical Biol. Med. 32 (2002) 1076–1083.
[59] D.G. Smith, R. Cappai, K.J. Barnham, Biochim. Biophys. Acta 1768 (2007) 1976–1990.
[60] M. Nakamura, N. Shishido, A. Nunomura, M.A. Smith, G. Perry, Y. Hayashi, K. Nakayama, T. Hayashi, Biochemistry 46 (2007) 12737–12743.
[61] C.X. Xie, M.P. Mattson, M.A. Lovell, R.A. Yokel, Brain Res. 743 (1996) 271–277.
[62] A. Khan, J.P. Dobson, C. Exley, Free Radical Biol. Med. 40 (2006) 557–569.